Topography-Based Registration of Developing Cortical Surfaces in Infants Using Multidirectional Varifold Representation

Islem Rekik, Gang Li, Weili Lin, and Dinggang Shen*

Department of Radiology and BRIC,
University of North Carolina at Chapel Hill, NC, USA
dgshen@med.unc.edu

Abstract. Cortical surface registration or matching facilitates atlasing, cortical morphology-function comparison and statistical analysis. Methods that geodesically shoot surfaces into one another, as currents or varifolds, provide an elegant mathematical framework for generic surface matching and dynamic local features estimation, such as deformation momenta. However, conventional current and varifold matching methods only use the normals of the surface to measure its geometry and guide the warping process, which overlooks the importance of the direction in the convoluted cortical sulcal and gyral folds. To cope with the stated limitation, we decompose each cortical surface into its normal and tangent varifold representations, by integrating principal curvature direction field into the varifold matching framework, thus providing rich information for the direction of cortical folding and better characterization of the cortical geometry. To include more informative cortical geometric features in the matching process, we *adaptively* place control points based on the surface topography, hence the deformation is controlled by points lying on gyral crests (or "hills") and sulcal fundi (or "valleys") of the cortical surface, which are the most reliable and important topographic and anatomical landmarks on the cortex. We applied our method for registering the developing cortical surfaces in 12 infants from 0 to 6 months of age. Both of these variants *significantly* improved the matching accuracy in terms of closeness to the target surface and the precision of alignment with regional anatomical boundaries, when compared with several state-of-the-art methods: (1) diffeomorphic spectral matching, (2) current-based surface matching and (3) original varifold-based surface matching.

1 Introduction

Advancing our understanding of the cerebral cortex development, neuroplasticity, aging and disorders is of tremendous value in modern neuroscience and psychology. The ever-growing acquisition of neuroimaging datasets mined for morphometric and functional brain studies continues to churn out wide spectrums of computational neuroanatomy methods. In particular, registration methods have been exhaustively developed in order to better align the imaging data

* Corresponding author.

N. Navab et al. (Eds.): MICCAI 2015, Part II, LNCS 9350, pp. 230–237, 2015.
DOI: 10.1007/978-3-319-24571-3_28

to a common space, where statistical analyses can be performed. Due to the remarkable convolution and inter-subject variability of cortical foldings, volume-based warping typically produced poorly aligned sulcal and gyral folds [1]. In contrast, cortical surface-based registration can better align the convoluted and variable cortical folding, owing to respecting the inherent topological property of the cortex during registration. Recently, Lombaert *et al.* incorporated more local geometric features in an *exact* surface matching framework, which estimated a diffeomorphic correspondence map *via* a simple closest neighbor search in the surface spectral domain [2]. Its accuracy measured up to the performance of Freesurfer [3] and Spherical Demons [4]. However, both of these methods [3,4] do not directly operate on the cortical surface, as they inflate each cortical hemisphere into a sphere and then register them in the spherical space, which inevitably introduces distortion to surface metrics.

On the other hand, *inexact* surface matching methods, based on geodesically shooting one surface into another, present a spatially consistent method for establishing diffeomorphic correspondences between shapes and measuring their dissimilarity. In [5], the *current metric* provided groundwork for developing a generic diffeomorphic surface registration and regression model without having to establish the point-to-point surface landmark correspondence on the longitudinal shapes. One key strength of this mathematical model is that it measures dissimilarities between complex shapes of different dimensions such as distributions of unlabelled points (e.g. anatomical landmarks), curves (e.g. fiber tracts) and surfaces (e.g. cortices); thereby, *simultaneously and consistently* tracking local deformations in a set of *multi-dimensional shapes* within a large deformation morphometric mapping (LDDMM) framework. One drawback of this method is that it annihilates the sum of two shapes with opposing normals. Recently, Charon *et al.* in [6] solved this problem by proposing the use of the *varifold metric* –a variant of the current metric– for matching shapes with inconsistent orientations. Surfaces are encoded as a set of non-oriented normals, which are embedded into a space endowed with the varifold dissimilarity metric.

However, the conventional varifold matching framework developed in [6,7] does not consider the principal curvature direction of the deforming surface, whereas this represents a key feature of the convoluted cortical surface by encoding the local direction of sulcal and gyral folds that marked previous work on the cortex [8]. In this paper, we propose a novel surface matching method by extending the previous work of [6] and [7] for integrating topography-based surface features to achieve a more anatomically consistent and accurate matching of cortical surfaces in infants with dynamic cortex growth. First, we automatically and adaptively lay the control points on the cortex high hills (gyral crests) and deep valleys (sulcal fundi) through a supervertex surface partition for guiding the shape deformation from a source surface to a target surface. Second, we add a novel varifold surface representation encoded by its principal curvature direction, which will be combined to its normal varifold representation to solve a variational problem leading to a gradient shape matching. Finally, we compare the accuracy of our method with: (1) diffeomorphic spectral cortical matching [2], (2) current-based surface

matching [5], and (3) original varifold-based surface matching methods [6,7] in terms of geometric concordance between target and warped shapes and alignment with the boundaries of anatomical cortical regions.

2 Varifold-Based Surface Matching

The concept of varifold in geometric measure theory was recently used to solve shape matching problems in [6,7]. We begin by reviewing the basic concepts for matching two shapes using the varifold metric as exposed by [6,7].

Surface Representation as a Varifold. In the varifold framework, a surface S is embedded in a vector space E (here $\mathbb{R}^3$) and encoded by a set of its *nonoriented* normals $n(x)$ attached at each of its vertices x (Fig. **1**). These nonoriented vectors belong to the Grassman manifold $G_d(E)$ (the space of non-oriented tangent spaces), which in the case of surfaces, is defined as the quotient of the unit sphere $\mathbb{S}$ in $\mathbb{R}^3$ by two group elements $\{\pm Id_{\mathbb{R}^3}\}$. This quotient space $G_d(E)$ contains elements u that are equivalent to $u/|u|$ and $-u/|u|$, denoted as $\overleftrightarrow{u}$. Any surface is thereby represented as a distribution of non-oriented spaces tangent to each of its vertices and spread in the embedding space E.

In a similar construction of currents, a varifold surface is defined as a continuous linear form that integrates a vector field $\omega \in W$: $S(\omega) = \int_{\Omega_S} \omega(x, \overleftrightarrow{n(x)})|n(x)|dx$. The vector space W is defined as a Reproducing Kernel Hilbert Space (RKHS) on the square-integrable space $C_0(E \times G_d(E))$. The reproducing kernel k on the space of varifolds is the tensor product of kernels on E and on $G_d(E)$: $k = k_e \otimes k_t$, where k_e denotes a positive continuous kernel on the space E (same as currents) and k_t denotes an additional linear continuous kernel of non-oriented vectors on the manifold $G_d(E)$. In particular, for $x, y \in E$ and $\overleftrightarrow{u}, \overleftrightarrow{v} \in G_d(E)$, the varifold kernel is defined as $k((x, \overleftrightarrow{u}), (y, \overleftrightarrow{v})) = k_e(x, y)\left(\frac{u^T v}{|u||v|}\right)^2$, where $k_e(x, y) = exp(-|x-y|^2/\sigma_e^2)$ is a Gaussian scalar kernel that decays with a rate σ_e. This kernel parameter controls the scale under which geometric details are ignored when measuring the surface using the varifold metric. The space of varifold is then defined as the *dual* space W^* (*i.e.* the space of linear mappings from W into $\mathbb{R}$). By the reproducing property, any varifold in W^* is defined as: $\omega(x, \overleftrightarrow{u}) = \delta_{(x, \overleftrightarrow{u})}(\omega) =< k((x, \overleftrightarrow{u}), \cdot), \omega >_W$, where $\delta_{(x, \overleftrightarrow{u})}$ defines a Dirac varifold that acts on ω. A surface S with N meshes (triangles) is then approximated by the sum of Dirac varifolds parameterized by the positions x_i of the centers of its meshes and their corresponding normals: $S = \sum_{i=1}^{N} \delta_{(x_i, \overleftrightarrow{n_i})}$. The Dirac varifold does not depend on the orientation given to each triangle. More importantly, the varifold space is endowed with a dot-product that induces a norm used for measuring the difference between pairs of shapes $S = \sum_i \delta_{(x_i, \overleftrightarrow{n_i})}$ and $S' = \sum_j \delta_{(x'_j, \overleftrightarrow{n'_j})}$:

$$< S, S' >_{W^*} = \sum_i \sum_j k_e(x_i, x'_j) \frac{(n_i^T n'_j)^2}{|n_i||n'_j|} \tag{1}$$

Varifold Registration Using LDDMM. Geodesically shooting a source varifold S_0 onto a target varifold S_1 is fully defined by the initial momenta of

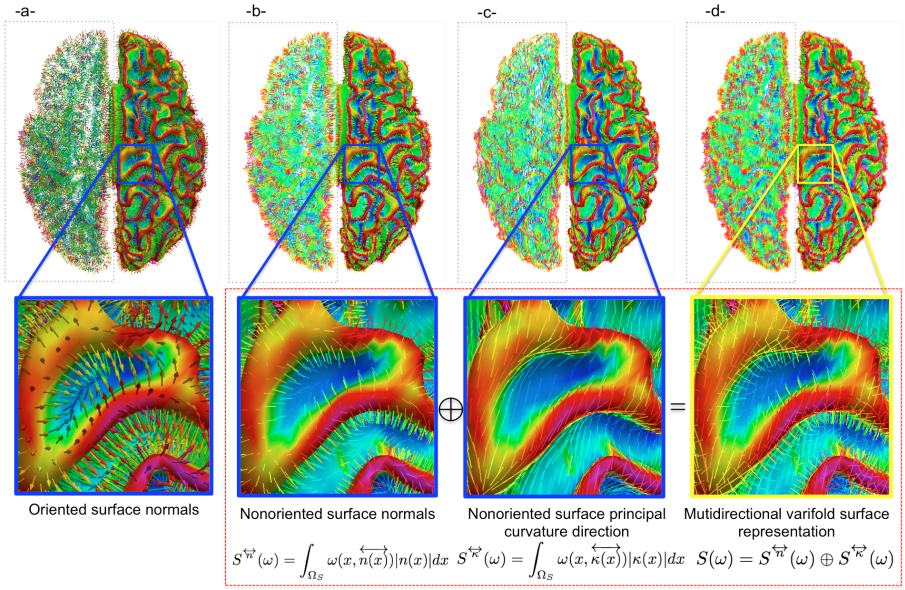

Fig. 1. *Cortical surface representations.* (a) The surface is represented using its oriented normals located at the centers of its meshes (*i.e.* a current) or (b) using its nonoriented normals (*i.e.* a varifold). (d) We propose to represent the surface S as a sum of two directional varifolds ($S^{\overleftrightarrow{n}}$ and $S^{\overleftrightarrow{\kappa}}$): one generated by its nonoriented normals (b) and the other by the nonoriented principal curvature direction (c).

deformation p_0. Geodesics (optimal deformation trajectories) are the solution of the flow equation: $\frac{d\phi_t(x)}{dt} = v_t \circ \phi_t(x), \quad t \in [0,1]$ with $\phi_0 = Id_{\mathbb{R}^3}$. ϕ_t is the diffeomorphism which acts on each mesh center x of S_0 to deform into $S_1 = \phi_1 \cdot S_0$. The time-varying deformation velocity v_t belongs to the RKHS V, densely spanned by a reproducing Gaussian kernel k_V which decays at a rate σ_V (the scale under which there is no deformation). In [7], the dense deformation was guided by a set of *control points* $\{c_k\}_{k=1,\ldots,N_c}$ that are estimated along with the initial momenta of deformation and the positions of the vertices in the warped surface. The velocity at any point $x \in E$ is defined as the sum of the scalar functions k_V (located at a set of control points $\{c_k\}_{1,\ldots,Nc}$) convoluted with their deformation momenta $\{p_k\}$: $v(x) = \sum_{k=1}^{N_c} k_V(x, c_k)p_k$.

Objective Functional. The estimation of the optimal initial deformation momenta, optimal control points and optimal warped vertices' positions is achieved through minimizing the following energy functional:

$J = \frac{1}{2}\int_0^1 |v_t|_V^2 dt + \gamma||\phi_1^v \cdot S_0 - S_1||_{W^*}^2$

The first energy term forces the warping trajectory to be smooth and the second makes the trajectory end close enough to the target surface. The parameter γ defines the trade-off between both of these terms. The objective functional J is minimized through a gradient descent algorithm as in [7].

3 Topography-Based Cortical Surface Matching Using Varifold Metric

Surface Multidirectional Varifold Representation. To better guide the geometric varifold warping, we propose a novel formula for surface varifold representation by adding the principal curvature direction κ: $S(\omega) = S^{\overleftrightarrow{n}}(\omega) \oplus S^{\overleftrightarrow{\kappa}}(\omega)$, where $S^{\overleftrightarrow{n}}(\omega) = \int_{\Omega_S} \omega(x, \overleftrightarrow{n(x)})|n(x)|dx$ and $S^{\overleftrightarrow{\kappa}}(\omega) = \int_{\Omega_S} \omega(x, \overleftrightarrow{\kappa(x)})|\kappa(x)|dx$.

Decomposing the surface into both of these 'orthogonal' components means that, instead of *reading* the shape of a surface in one direction using only the set of normals associated with its meshes, we perform an additional tangential reading in the principal curvature direction; thereby, collecting more geometric features that help register cortical surfaces through capturing important orientation information of cortical folding (Fig. **1**). However, unlike the computation of surface normals, the estimation of the principal direction is challenging as it may be noisy and ambiguous at flat cortical areas where both minimum and maximum principal curvatures are very small (Fig. **2**). To solve this problem, we first compute the principal directions and curvature derivatives using an efficient finite difference method. Second, we adopt a robust method developed in [9] to estimate smooth principal curvature directions that uniformly point towards the direction parallel to its folds –without diverting them from the original principal direction field. These are estimated through solving the variational diffusion equation: $E_d = \int_{\Omega_S} |\nabla\kappa(x)|^2 + f(x)|\kappa(x) - \eta(x)|^2 dx$ with respect to $\kappa(x) \cdot n(x) = 0$; where η denotes the original principal curvature direction, κ represents the diffused principal curvature direction, and $f(x)$ is set to the absolute value of the principal curvature at each vertex x. This propagates reliable and informative principal directions at sulcal bottoms and gyral crests to flat regions with unreliable principal directions, thereby generating a smooth tangential varifold which provides rich information of cortical folding. Subsequently, the varifold dot-product between two surfaces S and S' becomes:

$$< S, S' >_{W^*} = \frac{1}{2} \sum_i \sum_j k_e(c_i, c'_j) \frac{(n_i^T n'_j)^2}{|n_i||n'_j|} + \frac{1}{2} \sum_i \sum_j k_e(c_i, c'_j) \frac{(\kappa_i^T \kappa'_j)^2}{|\kappa_i||\kappa'_j|}$$

Topography-Based Control Points Selection. Instead of estimating the optimal control points near the most variable parts of the mean shape for both source and target shapes during energy minimization as in [7], we explore the highly variable topography of the cortical surface and adaptively place them on high gyral crests and low sulcal fundi. This allows for better exploration of the topography in the deforming cortical surface. We then feed them as inputs to the objective functional J. For this purpose, we adopt the supervertex cortical surface partition method developed by [10]. Supervertices seeds are uniformly placed on cortical surface and then a partition, that aligns the supervertices boundaries with gyral crests and sulcal fundi, is generated via minimizing an energy function using graph cuts. For our application, we choose to place the control points in cortical areas that will guide the deformation of the multidirectional surface varifold around each supervertex edge located at gyral crests and sulcal bottoms of the cortical surface by automatically checking the maximum principal curvature value (Fig. **2**).

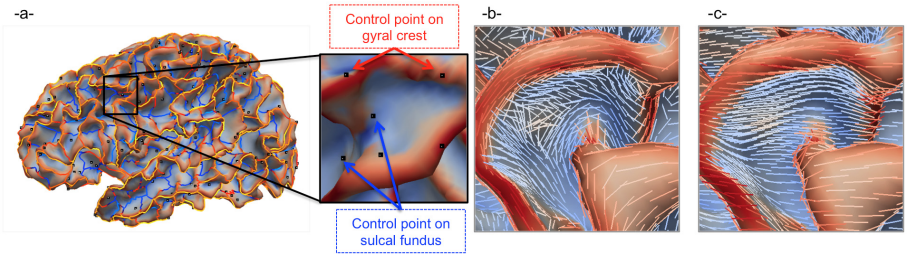

Fig. 2. *Key elements of the proposed method.* (a) Surface partition into supervertices and the control point placement on gyral crests and sucal fundi. Noisy principal direction (b) transformed into a smooth principal direction field (c).

Objective Functional. To estimate the initial momenta of deformation attached to each topographic control point placed on the target surface, we now minimize the following new energy using the numerical scheme proposed in [7]:

$$J_{new} = \frac{1}{2}\int_0^1 |v_t|_V^2 dt + \gamma_n ||\phi_1^v \cdot S_0^{\overleftrightarrow{n}} - S_1^{\overleftrightarrow{n}}||_{W*}^2 + \gamma_\kappa ||\phi_1^v \cdot S_0^{\overleftrightarrow{\kappa}} - S_1^{\overleftrightarrow{\kappa}}||_{W*}^2$$

4 Results

Data and Parameters Setting. We evaluated the proposed framework on inner cortical surfaces of 12 infants, each with MRI scans acquired at around birth and 6 months of age. We empirically fixed the current and varifold parameters at the same values for all infants: $\sigma_e = 5$, $\sigma_V = 20$ and $\gamma = 0.1$. For the novel varifold matching framework, we set $\gamma_n = 0.1$ and $\gamma_\kappa = 0.2$ to assign more weight to the fidelity-to-data term, depending on the surface principal curvature direction. In our experiments, we only used the minimum principal curvature direction which traces the gyral folding as a line.

Table 1. *Matching accuracy for twelve 0-to-6 month cortical surfaces.*

12 infants	Vertex-wise distance error (mm)	Average Dice over 36 ROIs
Spectral diffeomorphic exact matching	–	0.86 ± 0.004 ($p = 0.001$)
Current-based surface matching	1.15 ± 3.14	0.86 ± 0.03 ($p = 0.0002$)
Original varifold-based surface matching	0.64 ± 0.73	0.87 ± 0.015 ($p = 0.002$)
Proposed varifold-based surface matching	$\mathbf{0.60 \pm 0.65}$	$\mathbf{0.88 \pm 0.006}$

Benchmark with Three State-of-the Art Methods. We compared the results of the proposed method with: (1) diffeomorphic spectral cortical matching[1] where we used the mean curvature as a feature to refine the registration as pinpointed in [2], (2) current-based surface matching [5], and (3) original varifold-based surface matching methods[2] [6,7]. To evaluate the matching performance, we used two different criteria: (i) Euclidean distance (in mm) between the warped and the target

[1] The source code was kindly shared by first author in [2]

[2] We thank deformetrica research team for sharing the current-based and varifold-based matching code at `http://www.deformetrica.org/`

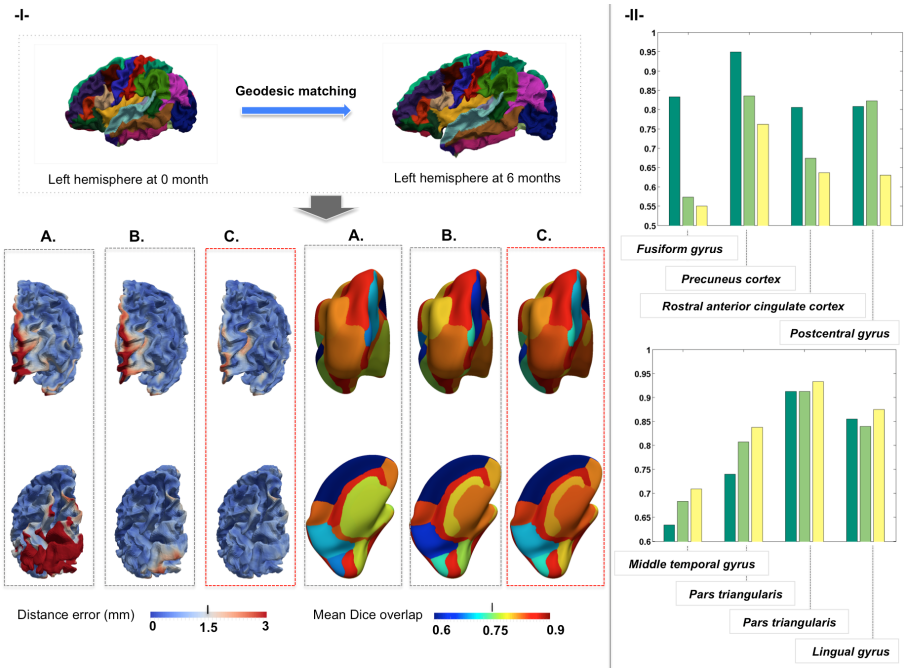

Fig. 3. *Euclidean distance error between the warped and the target hemispheres (left) and mean Dice overlap between warped and target parcellated hemispheres into 36 anatomical regions (right), both averaged across all subjects.* We overlay the average distance and mean Dice maps on a template for the current-based matching method (I-A), the original varifold matching method (I-B), and the proposed method (I-C). Bar plots represent the mean distance error (II-top) and mean Dice index (II-bottom) averaged across subjects in multiple highly folded and variable cortical areas for current (dark green), original varifold (light green) and proposed method (yellow). Our proposed method shows the best performance for (I-left) and performs at least as good as methods (A) and (B) and better in the majority of cortical areas for (I-right).

surfaces; and (ii) the accuracy of alignment with target anatomical region boundaries measured using the mean Dice area overlap index $d(S, S') = \frac{2|S \cap S'|}{|S|+|S'|}$ over 36 anatomical cortical regions. Table **1** shows that the proposed method achieves the best performance *w.r.t* both criteria. Our performance has improved with a rate similar to the Dice overlap ratios reported in [2] when compared to FreeSurfer and Spherical Demons. This improvement is notably visible in Fig. **3**, which displays the distance error map between the warped and the target surfaces and the mean Dice ratio between warped and target 36 boundaries of anatomical regions averaged across all subjects. The matching performance gradually ameliorates from the current-based method (Fig. **3**–I-A) to the original varifold method (Fig. **3**–I-B) and reaches its apex for the proposed method (Fig. **3**–I-C). The proposed method also outperforms other methods significantly in some highly variable and folded cortical regions (e.g. precuneus cortex and rostral anterior cingulate cortex) (Fig. **3**–II).

5 Discussion and Conclusion

We presented the first cortical surface registration method involving multiple directions for surface representation using the varifold metric and guided by topographic control points lying on the highs and the dips of the surface. Notably, the proposed framework capitalizes on a rich topographic and orthogonal reading of the deforming surface, applied for the first time to developing infant brains. Through surpassing the performance of several other state-of-the art surface registration methods, our proposed method can be used for building cortical surface atlases and better examining subjects with abnormal cortical development.

References

1. Thompson, P., Toga, A.: A surface-based technique for warping three-dimensional images of the brain. IEEE Trans. Med. Imaging 15, 402–417 (1996)
2. Lombaert, H., Sporring, J., Siddiqi, K.: Diffeomorphic spectral matching of cortical surfaces. Inf. Process. Med. Imaging 23, 376–389 (2013)
3. Fischl, B., Sereno, M., Tootell, R., Dale, A.: High-resolution intersubject averaging and a coordinate system for the cortical surface. Hum. Brain Mapp. 8, 272–284 (1999)
4. Yeo, B., Sabuncu, M., Vercauteren, T., Ayache, N., Fischl, B., Golland, P.: Spherical demons: fast diffeomorphic landmark-free surface registration. IEEE Trans. Med. Imaging 29, 650–668 (2010)
5. Durrleman, S., Pennec, X., Trouvé, A., Ayache, N.: Statistical models of sets of curves and surfaces based on currents. Medical Image Analysis 13, 793–808 (2009)
6. Charon, N., Trouvé, A.: The varifold representation of non-oriented shapes for diffeomorphic registration. SIAM Journal on Imaging Sciences 6, 2547–2580 (2013)
7. Durrleman, S., Prastawa, M., Charon, N., Korenberg, J., Joshi, S., Gerig, G., Trouvé, A.: Morphometry of anatomical shape complexes with dense deformations and sparse parameters. Neuroimage 101, 35–49 (2014)
8. Boucher, M., Evans, A., Siddiqi, K.: Oriented morphometry of folds on surfaces. Inf. Process. Med. Imaging 21, 614–625 (2009)
9. Li, G., Guo, L., Nie, J., Liu, T.: Automatic cortical sulcal parcellation based on surface principal direction flow field tracking. NeuroImage 46, 923–937 (2009)
10. Li, G., Nie, J., Shen, D.: Partition cortical surfaces into supervertices: Method and application. In: Levine, J.A., Paulsen, R.R., Zhang, Y. (eds.) MeshMed 2012. LNCS, vol. 7599, pp. 112–121. Springer, Heidelberg (2012)